A Rationale for the Absolute Conservation of Asn^{70} and Pro^{71} in Mitochondrial Cytochromes *c* Suggested by Protein Engineering†

Carmichael J. A. Wallace*,‡ and Ian Clark-Lewis§,||

Department of Biochemistry, Dalhousie University, Halifax, Nova Scotia B3H 4H7, Canada, and Biomedical Research Centre, University of British Columbia, Vancouver, British Columbia V6T 1W5, Canada

Received July 1, 1997; Revised Manuscript Received September 4, 1997⊗

ABSTRACT: The absolutely conserved residues Asn^{70} and Pro^{71} of mitochondrial cytochrome *c* have been targeted for protein engineering by semisynthesis. Neither residue has even been implicated in mechanistic schemes, and we reasoned that the conservation of this dipeptide was to fulfill a crucial structural role. Semisynthesis was through condensation by autocatalytic fragment religation of natural fragment 1−65 (H) of the horse protein and synthetic 39-residue peptides containing noncoded amino acids prepared by solid-phase methods. High yields of the purified analogs, homoserine^{70} and norvaline^{71} cytochromes *c*, were obtained. Functional tests revealed minor destabilization of the Hse^{70}-containing structure, with little adverse effect in *in vitro* assays, but [Nva^{71}] cytochrome *c* was essentially devoid of activity in these systems. This appeared to be a consequence of a shift, more pronounced than any yet reported, in the conformational equilibrium between the active state III conformer and the inactive, 'alkaline' state IV. The results support our view that this dipeptide is optimal for, and rigidifies, the right-angle bend between two α-helices, thus determining the conformation of the 70s loop that terminates in the sixth ligand Met^{80}, and 'forcing' the coordination of iron by thioether sulfur in the presence of the adjacent more avid amine ligands of state IV. Not only is [Nva^{71}] cytochrome *c* inactive at pH 7, but it also proves to be an extremely potent inhibitor of electron transfer by native state III, thus providing the rationale for the evolutionary conservation of a high p*K* for the ligand exchange reaction.

Evolutionary invariance is perhaps the primary clue used by protein scientists to identify amino acid residues making important contributions to protein structure and function and which in consequence are prime targets for protein engineering studies. For mitochondrial cytochrome *c*, primary sequences from more than 100 species are known (*1*). Of the 103−112 amino acids in these proteins, only 21 remain absolutely conserved, and most have been targeted for engineering by both semisynthetic (*2*) and genetic (*3*) approaches. One of the absolutely conserved residues is proline^{71}. Since its side chain offers no distinctive chemical attributes but does have unique structural properties, its role is related to the conformational integrity of the cytochrome fold, a motif common to both mitochondrial and the more variable prokaryotic cytochromes *c* (*4*). Its neighbor in the sequence, asparagine^{70}, is also highly conserved. Only one deviation, Asn → Asp, has been noted, in the *Drosophila* DC3 gene sequence (*5*). Although not a pseudogene, its transcript is found only at low and constitutive levels, and the corresponding protein has not been detected. The major *Drosophila* cytochrome *c* gene, DC4, has asparagine at position 70 (*5*), so this residue is effectively absolutely conserved. Thus, the possibility is raised that these two residues play a concerted, and crucial, role in maintaining the fold. Figure 1 illustrates the position of these two residues in relation to their neighbors and the heme group that is central to the cytochrome fold.

Some statistical and small molecule conformational studies may have relevance to this role. The most obvious relationship is to the 'Asx-turn' (*6*, *7*), a 10- or 13- member turn, observed in many proteins, completed by a hydrogen bond between the oxygen of the side-chain carbonyl of residue *i* and the main-chain amide of *i*+2 (or rarely, *i*+3) (*6*). The sequence that most favors this turn is *i* = Asn, *i*+1 = Pro. Detailed crystal structures of cytochromes *c* from several species are known, but none of them show an *i* to *i*+2 hydrogen bond, although *i* to *i*+3 H-bonds are described for the reduced yeast (*8*) and oxidized horse proteins (*9*). However, in every case, this pair of residues participates in an approximately right-angle bend between the two α-helical stretches 60−70 and 70−75, leading to the suspicion that there is a requirement for a rigid and kinked tubular structure at this point in the fold, and this dipeptide optimizes its stability. This arrangement may also stabilize the helices themselves. Amino acid preferences at the ends of α-helices have been analyzed (10). The most striking statistic to emerge is that there is a 3.5:1 preference for Asn at the 'N-cap' of a helix and a 2.6:1 preference for Pro at N-cap +1. Furthermore, the second most favored residue (after Gly) at the 'C-cap' is Asn, and Pro again is most preferred at C-cap +1.

Thus, we hypothesize that a 3-fold drive to utilize Asn-Pro to favor helix formation and/or stabilization at both N- and C-caps of abutting helices, and in the turn that establishes the right angle between them, finds expression in the absolute

† This work was supported by the Natural Sciences and Engineering Research Council of Canada, the Medical Research Council of Canada, and the Protein Engineering Network of Centres of Excellence of Canada.

* To whom correspondence should be addressed. Fax: (902) 494-1355. Email: cwallace@is.dal.ca.

‡ Dalhousie University.

§ University of British Columbia.

|| I.C.-L. is the recipient of an MRC Scholarship.

⊗ Abstract published in *Advance ACS Abstracts,* November 1, 1997.

S0006-2960(97)01595-X CCC: $14.00

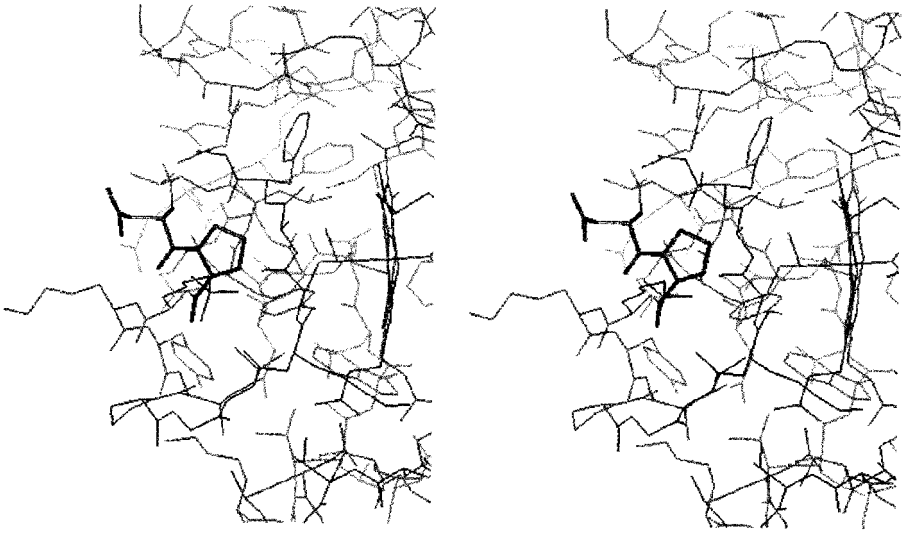

FIGURE 1: Stereoscopic view of the center of the conventional left side of the cytochrome *c* molecule from horse, emphasizing the two residues subject to mutation. Note also the proximity of the proline residue 71 to Met[80], between it and the heme group, and the position of the side chain of Lys[79], thought to be the major replacement ligand for Met[80] in the Nva[71] mutant at pH 7.

conservation of this element. We set out to test that hypothesis by considered substitutions of both residues and, since the most appropriate replacement side chains are noncoded, used semisynthesis to prepare the analogs.

One mutant of residue 70 has recently been reported but not yet characterized (*11*), and partially functional revertants of the nonfunctional [Leu[71]] mutant of *Saccharomyces* iso-1 cytochrome *c* have been identified (*11*, *12*). Some were used in estimations of the change in stability induced by mutation (*13*). A parallel study was made of a site-directed mutant of the iso-2 gene of yeast, in which threonine replaced Pro[71] (*14*). The [Val[71]], [Thr[71]], and [Ile[71]] cytochromes *c* have also been examined by X-ray crystallography, and small deviations from wild-type structure attributable to increased side-chain bulk were observed (*15*). We have extended these studies by detailed examination of physicochemical and biological properties and molecular modeling of the [Nva[71]] mutant, and looked at the behavior of the [Hse[70]] analog.

The observed consequences of the replacement of Asn[70] are relatively minor, but the Pro[71]→Nva substitution produces change in many primal characteristics of cytochrome *c* of a magnitude previously unobserved. We interpret these results in terms of a destabilization, which permits facile ligand exchange, of the secondary structural element described above. In addition, we show that the analog becomes a potent inhibitor of electron transport in the intact respiratory chain, offering a simple explanation of the extreme evolutionary conservatism of the Asn-Pro motif.

EXPERIMENTAL PROCEDURES

Peptide Synthesis, Protein Semisynthesis, and Product Purification. Established procedures were employed to prepare two 39-residue peptides (representing amino acids 66−104) by solid-phase synthesis and to religate them with the natural horse cytochrome *c* heme-containing fragment 1−65 (H) (*16*, *17*). Synthesis of the homoserine[70]- and norvaline[71]-containing peptides was exactly as described except that either N-tBoc-homoserine or N-tBoc-norvaline (Bachem Biosciences, Philadelphia, PA) was used in place of BocAsn or BocPro in the automated protocol (*17*). Purification of synthetic peptides employed preparative reverse-phase HPLC on a C18 matrix, with a subsequent analytical run on a C18 matrix as a control of purity. Products were checked both by amino acid analysis and by mass spectrometry. Semisynthetic cytochromes *c* were separated from unreacted fragments by size-exclusion chromatography followed by purification by cation-exchange chromatography. Product purity was subsequently checked by high-performance ion-exchange chromatography at an analytical scale (*16*). This methodology is also useful in detection of the change in net charge, or in surface charge distribution (dipole moment) of the product (*17*).

ATP-Binding Capacity. Cytochrome *c* binds a single ATP around physiological ionic strength at a location in the (conventional) upper left quadrant of the molecule. The ATP makes multiple contacts with the protein, stretching from Arg[91] and Lys[88] at one extreme to Ala[83] and Asn[70] at the other (*18*). The effect of the mutations at positions 70 and 71 on the strength of binding of ATP to the cytochrome was assessed by using an affinity column of ATP immobilized on an agarose gel as previously described (*19*).

Spectroscopic Studies of the Analogs. UV−visible spectra in both oxidation states were drawn from 750−250 nm on a Beckman DU65 spectrophotometer, and compared with those of native horse cytochrome *c*. The normal spectral state III of ferric cytochrome *c* can be perturbed by pH change. Spectral state transition to II (acid) or IV (alkaline) occurs with a characteristic p*K*, and includes complete loss of the 695 nm absorbance (*20*). This and other spectral changes imply a conformational change in the protein, and thus a measure of change in the stability of the native state is obtained by titration of the band with either decreasing or increasing pH (*21*, *22*).

Spectrophotometry is also used in the determination of oxidation−reduction potential by the method of mixtures, in which the ambient E'_m of a redox buffer is titrated and the change in redox state of a cytochrome dissolved in it is monitored (*22*).

Biological Assays. Two types of biological assay of mutant cytochromes were performed that use oxygen consumption determined potentiometrically as a measure of electron transfer rates. One of these is the succinate oxidase

assay in cytochrome *c*-depleted mitochondria, which we have described and discussed previously (*17*, *23*). The other assay employs purified cytochrome *c* oxidase. Preparation of the enzyme and details of the assay have been described (*24*). Tangents to the rate vs concentration curves (initial rates) are used as a comparator of electron transfer efficiency, in both assay systems, of the cytochromes tested: the use of this measure has been discussed (*23*).

A spectroscopic assay of the electron uptake rate by cytochrome *c* for the bc_1 complex (cytochrome *c* reductase) was also employed. A suspension of cytochrome *c*-depleted mitochondria (10 μL) prepared for the succinate oxidase assay above was diluted with 500 μL of the succinate-containing buffer, giving a reductase concentration of approximately 2 nM. To this mixture was added 10 μL of 100 mM KCN. Cyanide ion binds to oxidase heme and prevents reduction of O_2, but at this concentration reacts only very slowly with ferricytochrome *c* (*25*). The cytochrome *c* to oxidase transfer is thus inhibited, and upon addition of oxidized cytochrome *c* (50 μL of 0.25 mM), rapid reduction of the latter ensues that can be monitored as ΔA_{550}. Tangents to the curves recorded were used to obtain initial rates.

In addition to comparing mutant cytochromes to the parent protein in these assays, the inhibitory potential of [Nva^{71}] cytochrome *c* was assessed by using assay systems that had been repleted with near-saturating quantities of native cytochrome. Sequential additions of the Nva^{71} analog were made, and the fall in activity was noted after each addition. In the case of the reductase assay, a set of initial rates were also determined under conditions in which the total cytochrome concentration was kept constant, but the ratio of native to mutant cytochrome was varied.

The kinetics of ascorbate reduction of cytochromes *c* at 25 °C were followed in the DU65 spectrophotometer by the change in A_{550} after addition of an aliquot of ascorbic acid (50 μL of a 1 mg·mL^{-1} solution in water) to a cuvette containing 950 μL of a 35 or 17.5 μM solution of cytochrome *c* or analog in 50 mM phosphate buffer, pH 7. Progress curves for reduction were obtained using the spectrophotometer's kinetics program and half-times for complete reduction compared. Reoxidation of reduced cytochromes *c* was also followed in the same system after buffer exchange, on a short Sephadex G25 column, from an ascorbate-containing to an O_2-containing solution.

Molecular Modeling and Dynamics Simulations. A model of the Pro^{71}→Nva variant of horse cytochrome *c* was built based on the coordinates (*9*) obtained from the Brookhaven Protein Data Bank (entry no. 1HRC). The mutation from proline to norvaline was made in the model by breaking the bond between the backbone nitrogen and δ carbon of Pro^{71}, and adding a hydrogen atom to each of these heavy atoms. Water molecules observed from X-ray analysis were added to the model, and then further surrounded by a 5 Å layer of solvent water. This model was then energy-minimized with the programs Insight II and Discover (Biosym Technologies, San Diego, CA), using parameters for the heme group and methods taken from the previous molecular dynamics simulations (*19*).

The minimized model was subjected to a molecular dynamics run in order to search for different conformations of the Nva^{71} side chain. The potential energy function used was identical to that used for energy minimization, and the simulation was performed at a temperature of 300 K for 10 000 iterations.

RESULTS

Peptide Synthesis and Semisynthesis. High yields of purified synthetic 39-residue peptides (Hse^{70}, 104 mg; Nva^{71}, 217 mg) were obtained from 0.4 mmol of 1 mmol·g^{-1} loaded resin. Structures were confirmed by amino acid analysis and mass spectrometry. For the Hse^{70} peptide, the observed mass was 4559.6 ± 1.1 Da, compared to expected mass values of 4557.5 Da (monoisotopic) or 4560.4 Da (average). In the Nva^{71} case, the mass observed was 4574.8 ± 1.0 Da: expected 4572.5 Da (monoisotopic) or 4575.4 Da (average). These were combined with 1−65 (H) at good efficiency: 45% yield at equimolar fragment concentration. This value compares with 60−70% obtained with the natural fragment 66−104 or the synthetic fragment of native sequence. The semisynthetic strategy employed (*16*) leaves homoserine, not methionine, at position 65, but products from both natural and synthetic native fragment 66−104 are indistinguishable from the native protein in all functional tests.

Ion-Exchange Chromatography. A single passage on a preparative-scale Trisacryl SP cation-exchange column was adequate to separate pure cytochrome *c* analogs from the deamidated forms and fragment polymers that contaminated the crude preparations. Analytical high-performance cation-exchange chromatography of [Hse^{70}] cytochrome *c* showed two peaks only, with elution times of 13.3 and 14.3 min, compared with times of 13.2 and 14.1 min for horse ferrocytochrome and ferricytochrome, respectively. Even fully oxidized protein normally undergoes some reduction in the anaerobic HPLC system, but [Nva^{71}] cytochrome *c* gave a single peak of oxidized protein eluting at 12.9 min. Since formally this substitution involves no change in the net charge, the result may indicate a change in the dipole that is a consequence of conformational change in this highly polar protein (*17*).

Affinity Chromatography. Elution times in both gradient and isocratic systems for [Hse^{70}] and native cytochromes are essentially identical, but the ATP affinity of the Nva^{71} analog is much lower. Under isocratic conditions, this analog does not bind to the column, and it eluted at 19 min (native 29 min) in the gradient system. This indicates conformational change in the ATP binding site and, since the mutated side chain is not making contact with ATP, must be an indirect effect of the change. The ligand exchange reaction in the alkaline transition of cytochrome *c* is paralleled by a substantial drop in the affinity of ATP also (*26*).

UV−Visible Spectra. At pH 7, the spectrum of [Hse^{70}] cytochrome *c* did not differ from that of the native protein, but [Nva^{71}] cytochrome *c* showed marked deviations from the normal pattern in the ferric state, though the dithionite-reduced protein appeared quite normal. The α/β band was shifted from 528 to 530 nm, the Soret (γ) band from 410 to 404 nm and the δ band from 360 to 353 nm. Most remarkably, there was complete loss of the 695 nm band. Such a pattern is characteristic of spectroscopic state IV, the 'alkaline' form of the protein, though no previously described analog has been found to be completely in this state at pH 7.

Titration of the 695 nm Band. The result described above was confirmed by titration to pH 3 (Figure 2). It is clear

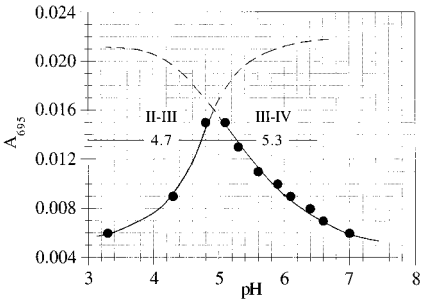

FIGURE 2: A_{695} versus pH for [Nva^{71}] cytochrome *c*. The spectrum of the mutant protein in 50 mM phosphate buffer, pH 7, was drawn and compared with those obtained on changing the pH by the addition of small volumes of 1 M HC1. The absorbance change at 695 nm is plotted and shows first an increase with decreasing pH as the Met S−Fe coordination forms, followed by a decrease at lower pH as the acid transition occurs. At the A_{695} maximum around pH 5, comparison with other absorption bands shows that this is not fully developed—the dotted lines show projected titration curves for both acid and alkaline transitions if the normal maximal absorbance of this band were achieved.

Table 1: Average Oxidation−Reduction Midpoint Potentials in Millivolts of Horse Cytochrome *c* and Semisynthetic Analogs at a Range of pH Values[a]

cytochrome	native horse	[Nva^{71}]	[Nva^{71}] corrected	[Hse^{70}]
pH 7	272−276	(136)	−	272
pH 6.5	−	(165)	−	−
pH 6	274	194	230	−
pH 5.5	−	203	227	−
pH 5	274	212	225	−

[a] For the native protein at pH 7, the range of values encountered in this study is shown. Corrected values for [Nva^{71}] cytochrome *c* are obtained by using Figure 2 to estimate the proportion of state III ferricytochrome *c* in the mixture at any pH value and adjusting the ferro- to ferricytochrome *c* ratio used in the calculation of E'_m accordingly. Values in parentheses at higher pH for [Nva^{71}] indicate that these data are less reliable due to the very small proportion of the reduced form in the mixture under these conditions.

from the figure that the transitions have p*K*s so close to one another that, as pH falls, the full development of the 695 nm band is not realized before the onset of the acid transition in which this band is once more lost. However, it seems reasonable to assume that were it possible for full development of the band to occur then it would have the same extinction coefficient as in the native protein and numerous other analogs. Using the characteristic curve for the alkaline transition (*21*) and the extinction coefficient of the native horse protein, we have extrapolated to full development of the band (Figure 2) and have by inspection estimated p*K*s (as the pH of half-development of the extrapolated 695 nm intensity) for the transitions. Comparable values for the native protein are 9.2 and 2.7. A similar titration with the [Hse^{70}] cytochrome gave values of 8.4 and 3.3.

Oxidation−Reduction Potentials. Potentials determined by the method of mixtures for both analogs are compared to those of the native protein (at a range of pH values in the case of the [Nva^{71}] protein), in Table 1. Although the [Hse^{70}] analog shows a normal E'_m, that of [Nva^{71}] increases with decreasing pH, although the value for the native protein is stable over the range pH 5−7. Since this is undoubtedly due to the increasing proportion of high potential state III in the mixture [state IV has a very low E'_m (*27*, *28*)], the redox titration data can be recalculated on the basis of the actual proportion of state III ferricytochrome present estimated by

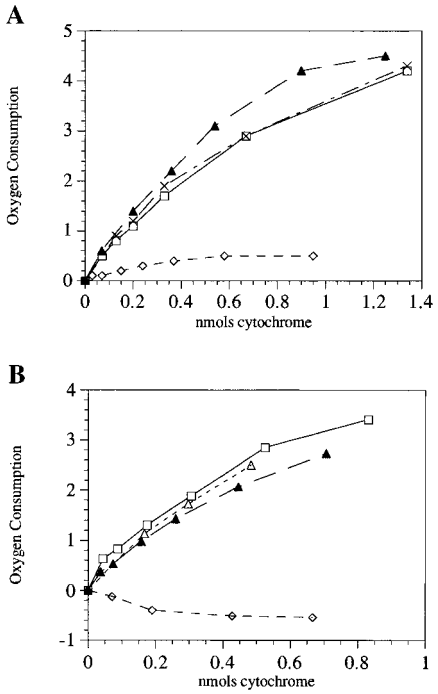

FIGURE 3: Biological assays of [Hse^{70}] and [Nva^{71}] cytochromes *c* compared with the native horse protein. (A) The depleted mitochondria succinate oxidase assay. (B) Isolated oxidase assay. The figures show O_2 consumption as percent of total dissolved O_2 per minute, versus amount of added cytochrome *c*; □ and ×, horse; Δ and ▲, [Hse^{70}]; ◇, [Nva^{71}].

comparing the actual 695 nm absorbance of the analog at that pH with that of native cytochrome *c*. A consistent, but low, value of E'_m for [Nva^{71}] cytochrome *c* in the state III conformation is thereby obtained.

Nonbiological Oxidation and Reduction. The UV−visible spectrum suggests that the major form of the [Nva^{71}] analog is the equivalent of state IV of cytochrome *c*, in which case it should only slowly be reduced by ascorbate. The half-time of reduction of cytochrome *c* at 35 μM in 50 mM phosphate buffer, pH 7, by 280 μM ascorbate is approximately 48 s. Decreasing the cytochrome *c* concentration to 17.5 μM increases $t_{1/2}$ by 6 s, while increasing the ionic strength to 250 mM phosphate (and thus decreasing the electrostatic interaction between basic cytochrome *c* and the anionic ascorbate) doubles $t_{1/2}$.

For the analogs, a significant increase to 91 s was noted for the [Hse^{70}] protein, and $t_{1/2}$ for [Nva^{71}] cytochrome *c* at pH 7 was 1380 s, which reduced to about 300 s at pH 5.5. Thus, both analogs in state III are somewhat more slowly reduced by ascorbate. After removal of ascorbate on a G25 column, oxidation of reduced [Nva^{71}] cytochrome was so rapid that it was complete before the sample emerged from the column at 5 min.

Biological Assays. A comparison of the abilities of the analogs to stimulate O_2 uptake in the succinate oxidase assay system is shown in Figure 3A. While the [Hse^{70}] protein has at least equivalent activity to the native protein, [Nva^{71}] cytochrome *c* has very substantially reduced electron transfer ability. In Figure 3B, results in the oxidase assay for this analog are presented. The apparent negative activity is a consequence of a depression of the normal low basal O_2 uptake in this system, which is due to direct reduction of the oxidase by ascorbate or TMPD. The implication of this depression by a presumably inactive protein is that non-

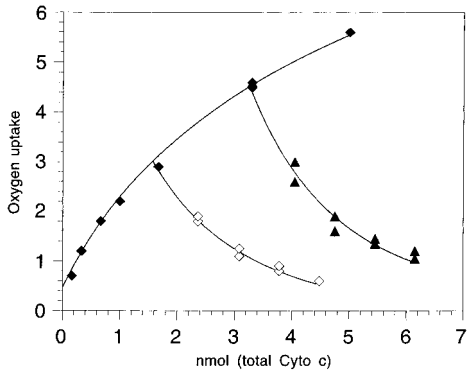

FIGURE 4: Assays of electron transport inhibition I. Effect of the addition of [Nva^{71}] cytochrome *c* upon oxygen uptake, as percentage of total dissolved O_2 per minute, stimulated by native horse protein in cytochrome *c*-depleted rat liver mitochondria. The upward curve is the standard for cytochrome *c* addition; the two curves descending from it represent the effect of replacing native protein by analog in further incremented additions, commencing at the junction points.

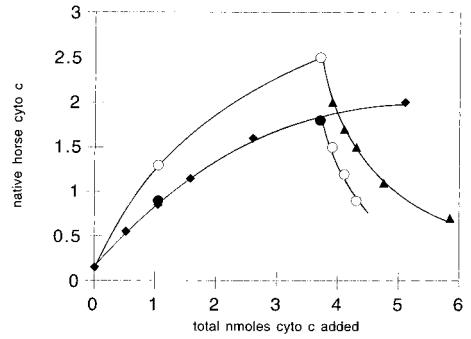

FIGURE 5: Assays of electron transport inhibition II. A similar protocol to that of Figure 6, but using isolated cytochrome oxidase in the assay, from two preparations of oxidase of slightly differing activity in upper and lower curves.

physiological reductants and cytochrome *c* share a common binding site on the oxidase. In this assay, too, [Hse^{70}] cytochrome *c* differs little in its properties from the native protein.

This indication that the Nva^{71} analog, though not competent in electron transfer, could yet bind strongly to oxidase and inhibit nonphysiological reduction was further investigated in a physiological context.

Native cytochrome *c* was added to cytochrome oxidase preparations under standard assay conditions (pH 7.5) until an O_2 uptake of approximately 80% of maximal was achieved (Figure 5). Addition of even small quantities of [Nva^{71}] cytochrome *c* at this point caused a precipitate drop in the electron transfer rate, indicative of tighter binding of analog than functional protein, and consequent very effective inhibition. To see if a similar effect was operative in the more 'in vivo' context of a complete respiratory chain, osmotically-shocked mitochondria were used. These have no outer membrane, so the intermembrane cytochrome *c* may be removed, but the inner membrane is intact, and phosphorylation-coupled respiration can be restored. The cytochrome *c*-depleted mitochondria were thus repleted with the native protein to levels that gave approximately 50 or 75% of maximal turnover. At this point, further additions of cytochrome were made, but of the inactive mutant. As Figure 4 shows, another extensive fall-off of activity occurred.

That the effect is not quite so dramatic as with the oxidase may be due to one of two reasons. This assay is performed at pH 7 where a higher fraction of the analog will be in the state III conformation than at pH 7.5. Additionally, with the succinate oxidase system, cytochrome *c* undertakes electron transfer with both oxidase and reductase, and sensitivities may differ. Therefore, we looked at electron transfer rates from reductase to cytochrome *c* alone by poisoning the oxidase with cyanide. Reduced cytochrome *c* accumulates, and the reduction rate can be monitored by the increase in 550 nm absorbance. At pH 7, with saturating amounts of cytochrome *c*, the electron acceptance rate of the analog is approximately 4% of that of wild-type. Furthermore, addition of analog to reductase−cytochrome *c* mixtures depresses the overall reduction rate substantially, but also less markedly than it does the rate of cytochrome *c* oxidation by purified oxidase (data not shown).

Computer Modeling of the Nva^{71} Substitution. The side chain of asparagine^{70} is exposed at the molecular surface and thus can be replaced by near-isosteric residues like homoserine with an expectation of limited steric consequences. However, even though norvaline was chosen as the closest homolog to proline^{71}, its buried location raises questions as to the conformational consequences in the tightly packed interior of the molecule. Figure 6 shows a comparison of the wild-type horse cytochrome *c* structure in the vicinity of this residue with that obtained by an energy minimization of all atoms in the structure after replacement of Pro^{71} by Nva, with a subsequent 10 ps molecular dynamics simulation. The comparison reveals that there is minimal alteration of protein conformation near the mutation site, or, indeed, elsewhere in the molecule, though in response to the increased bulk, and extended conformation of the norvaline residue, the 80s ridge appears to be displaced *en masse* slightly closer to the exposed heme edge (Figure 6).

DISCUSSION

Replacement side chains were chosen that would both abolish what was presumed to be the crucial structural aspects of the original side chain and conserve the essential physicochemical properties. Thus, for Asn^{70}→Hse, the same carbon skeleton is preserved, but the amide group is replaced by a single hydroxyl to alter the hydrogen-bonding potential while conserving polarity. In the Pro^{71}→Nva mutant, the replacement side chain is near-isosteric with three carbon atoms, but the cyclic nature of the original side chain is lost and additional hydrogen atoms are introduced at CD and N.

The global structural consequences, either internal or at the surface of the Asn^{70}→Hse substitution, are not great. Where the analog does differ from the native protein, though, is in the p*K*s of the spectroscopic transitions, but only by less than a single pH unit in each case. Thus, at pH 7 the protein remains fully functional. Neither reactivity with reductase nor reactivity with oxidase deviates much from the normal range. Although it is clear that the asparagine does make some contribution, through the specific hydrogen bond(s) that it can form, to the global stability of the protein, homoserine can provide a functional substitute, and so might other residues. Why then the extreme evolutionary conservatism? It is possible that even small changes in functional competence are strongly selected against over evolutionary time scales, or the assay conditions do not fully reflect

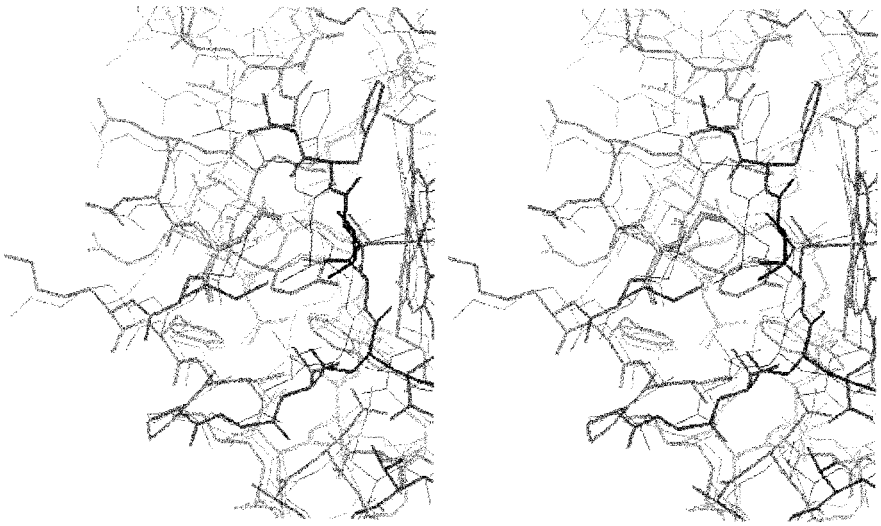

FIGURE 6: Stereoscopic view of a comparison of native and hypothetical analog structures in the heme crevice region. A superimposition of the crystal structure of the horse protein derived from the Brookhaven Protein Data Bank (thin lines) and that computed for the mutant (thicker lines) using the molecular dynamics procedure described under Experimental Procedures.

electron transport requirements in the potentially more stressful circumstances of authentic physiology. Alternatively, one could postulate that, as in the case of arginine[91] (*18*, *24*, *26*), this residue provides an important function not tested by considerations of electron transport alone.

No such uncertainties exist for the mutation of Pro[71]. The sweeping loss of functionality under standard conditions can almost entirely be correlated with an unprecedented shift in the p*K* of the "alkaline" transition, by 4 pH units, corresponding to a relative destabilization of the native conformation by 5.5 kcal·mol^{-1}. The apparent change in dipole moment monitored by cation-exchange HPLC indicates a significant difference in the surface conformation between native protein and analog, and/or loss of a single positive charge, and the single peak detected is a mark of the low redox potential of [Nva[71]] cytochrome *c*.

Likewise, the fall in ATP affinity noted for this analog is indicative of a surface conformational change that includes the site, and parallels the loss of affinity noted when the protein undergoes the alkaline transition. In addition to the loss of the 695 nm absorbance that accompanies the breaking of the $Fe^{III}-S$ bond, the other spectral properties at pH 7 indicate state IV and nitrogenous ligation of the ferric iron.

After many years of debate (*20*), it is now virtually certain that the replacement ligand is a lysine amino group (*28*). There prove to be two isomers of the alkaline form, in one of which lysine 79 provides the competing ligand. The other lysine has not been identified but is probably one of 73, 86, or 87. Inspection of the structures shown in Figures 1 and 7 reveals that a relatively minor upward ratcheting of the 77−85 strand would allow the former replacement, but that any of the other substitutions would demand a more substantial reorganization. Lysine ligation requires its prior deprotonation, and hence a reduction of the net charge of the protein as well as surface structural reorganization, so the substantial differences in ion-exchange and ATP-affinity chromatographic properties are consistent with this view, and both increasing pH around the native protein (*1*) and replacing methionine 80 with a nitrogenous ligand (ornithine; *17*) causes substantial falls in redox potential.

The balance of evidence overwhelmingly supports the view that the differences between this analog and the parent protein stem from the attainment, at a much lower pH than usual, of the well-characterized spectroscopic state IV of the cytochrome with lysine amino−iron ligation. In consequence, at pH 7.5, the pH of the oxidase assay, the protein is almost entirely in state IV, and not reducible by ascorbate/TMPD. The results of the inhibition assays show that the analog competes very strongly with the native protein, and imply that the conformational rearrangements provide a better fit to the recognition site that is located close to the binuclear copper center near the oxidase surface (*29*). Such a potent inhibitory effect provides the pressure for the strong evolutionary conservatism of the high p*K* of the ligand exchange reaction.

Correction of the redox potential calculation to reflect the actual proportion of high-potential state III conformer gives an E'_m value that still falls short of that of the native protein. The control of redox potential by the protein matrix enclosing the heme center is multifactorial (*17*), but in this case the change in potential is most likely to reflect a greater degree of solvent accessibility to the heme. Small-molecule accessibility is confirmed by the rapidity of oxidation by dissolved O_2. The changes observed by X-ray structural studies in Pro[71] mutants (*15*) are largely confined to the region of the polypeptide chain (82−84) that closes off the conventional 'top' of the heme crevice. Both displacement of this region and an increase in thermal factors were seen, and the molecular dynamics modeling we have done of the Nva[71] analog shows an even greater movement of this region (Figure 6).

If the functional changes can all be attributed to conformational destabilization, can we now explain how the Pro[71]→Nva side-chain substitution can have such a pronounced effect? The coordination of ferric heme iron by methionine sulfur is intrinsically a very weak interaction (*17*), so it is presumed that part of the polypeptide chain's role is to hold the methionine residue in place in the face of competing, stronger ligands, either protein-bound or extrinsic. An obvious element important to the position of this side chain is the 70s loop, and the initiating element of this loop is the turn between α-helices created by the Asn[70]-Pro[71] dipeptide (Figure 7).

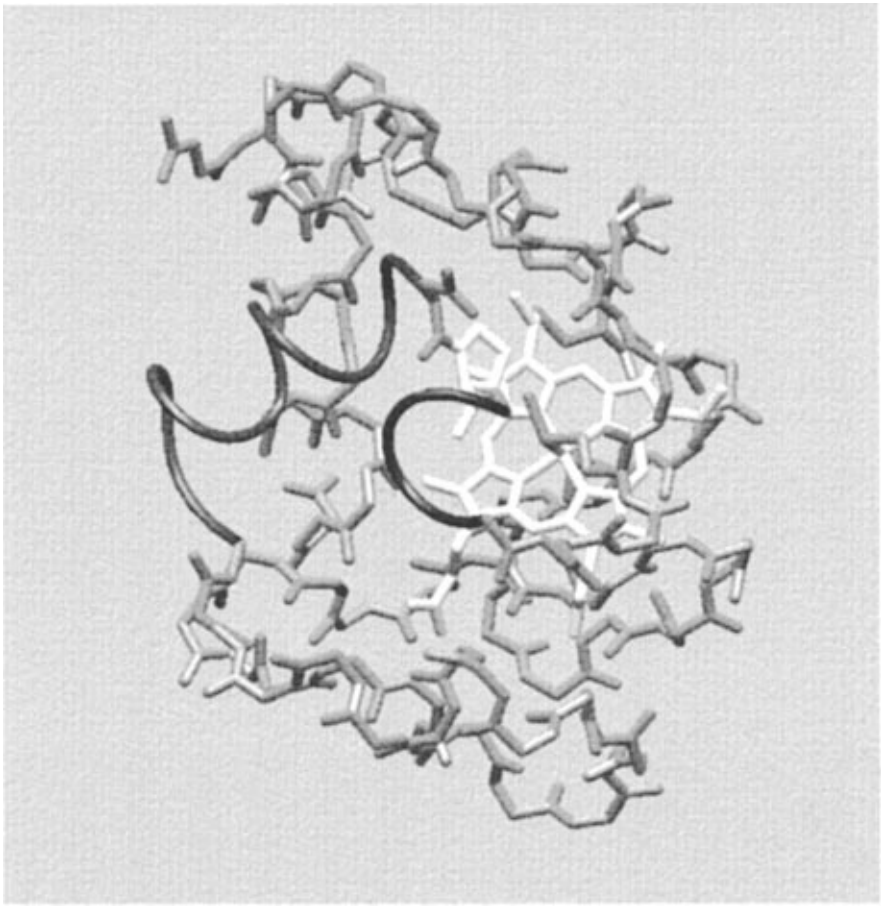

FIGURE 7: View of the relationship of the Asx turn under investigation to the α-helices that flank it. This form of representation emphasizes the fact that the turn defines a right-angle bend in the tubular structure, and so rigidifies the 70s loop, that commences at the bend, relative to the central heme group.

Thus, the primary role of the proline residue may be to provide, through the conformational rigidity imposed by its unique structure, an inflexible right angle to initiate the 70s loop structure and maintain the desirable methionine coordination. When it is replaced, greater flexibility in the loop would facilitate the ratcheting required to move into position the lysine 79 side chain required for ligand replacement, and loosen the 81−85 stretch to permit greater small-molecule access to the heme.

There is variability in the extent of change in pK_{695nm}, and of other spectral changes, with the nature of the replacement residue, in those mutants studied in the past (*13*, *14*, *30*). Transition p*K*s of close to or below 7 were reported for them, and that of the Leu^{71}-containing mutant may be comparable to the Nva^{71} analog, since the low growth rates of yeast containing it suggest complete lack of function (*12*). The extent of destabilization measured by this parameter is paralleled by that determined for guanidine hydrochloride-induced unfolding (*14*, *30*). In vitro measurements of electron-transfer kinetics have not been made, but relative growth rates of the yeast strains containing them indicate modest to moderate functionality (*12*). Levels of expression are normal (*11*).

The extreme functional derangement experienced in our Nva^{71} analog is thus probably not entirely due to relaxing the stiffness of the interhelical joint. The displacement in the 80s ridge noted in the modeling is more extreme than that demonstrated crystallographically for other mutants (*15*), and modeling of the presumed inactive Leu protein suggests a steric clash with residues 80 and 82 that would be likely to produce a similar effect. This shift may well facilitate the ligand exchange reaction and compound the destabilization. Nevertheless, the dominant factor in loss of function results from the primary role of proline in making the turn that defines the optimal conformation of the 70s loop for correct heme iron coordination. Any replacement of the proline residue will be inadequate in this role, as in the functional, but defective, [Val^{71}], [Ile^{71}], and [Thr^{71}] mutants, and thus no phylogenetic variability is observed. But norvaline (and, presumably, leucine) may for steric reasons compound this effect so that the destabilization of the heme crevice is complete at physiological pH and a totally nonfunctional protein results. As a consequence, a model of the state IV conformer of native cytochrome *c* is now available to us for structural, and further functional, analysis at pH 7.

ACKNOWLEDGMENT

We are very grateful to Dr. Jonathan Parrish for his invaluable assistance in preparing molecular models. We thank Anne Rich and Angela Brigley for valuable technical assistance, Phil Owen and Peter Borowski for help with the peptide synthesis, and Anthony Woods for help with preparation of some of the figures.

REFERENCES

1. Moore, G. R., and Pettigrew, G. W. (1990) *Cytochromes c: evolutionary, structural and physico-chemical aspects*, Springer-Verlag, Berlin.

2. Wallace, C. J. A. (1996) in *Cytochrome c: a multidisciplinary approach* (Scott, R. A., and Mauk, A. G., Eds.) pp 693−728, University Science Books, Sausalito, CA.
3. Lo, T. P., Guillemette, J. G., Louie, G. V., Smith, M., and Brayer, G. D. (1995) Biochemistry *34*, 163−171.
4. Salemme, F. R. (1977) Annu. Rev. Biochem. *46*, 299−329.
5. Limbach, K. J., and Wu, R. (1985) Nucleic Acids Res. *13*, 631−644.
6. Baker, E. N., and Hubbard, R. E. (1984) Prog. Biophys. Mol. Biol. *44*, 97−179.
7. Pichon-Pesme, V., Aubry, A., Abbadi, A., Boussard, G., and Marraud, M. (1988) Int. J. Pept. Protein Res. *32*, 175−182.
8. Louie, G. V., and Brayer, G. D. (1990) J. Mol. Biol. *214*, 527−555.
9. Bushnell, G. W., Louie, G. V., and Brayer, G. D. (1990) J. Mol. Biol. *214*, 585−595.
10. Richardson, J. S., and Richardson, D. C. (1988) Science *240*, 1648−1652.
11. Takakura, H., Yamamoto, T., and Sherman, F. (1997) Biochemistry *36*, 2642−2648.
12. Ernst, J. F., Hampsey, D. M., Stewart, J. W., Rackovsky, S., Goldstein, D., and Sherman, F. (1985) J. Biol. Chem. *260*, 13225−13236.
13. Ramdas, L., Sherman, F., and Nall, B. T. (1986) Biochemistry *25*, 6952−6958.
14. White, T. B., Berget, P. B., and Nall, B. T. (1987) Biochemistry *26*, 4358−4366.
15. Murphy, M. E. P. (1993) Ph.D. Dissertation, University of British Columbia.
16. Wallace, C. J. A., Mascagni, P., Chait, B. T., Collawn, J. F., Paterson, Y., Proudfoot, A. E. I., and Kent, S. B. H. (1989) J. Biol. Chem. *264*, 15199−15209.
17. Wallace, C. J. A., and Clark-Lewis, I. (1992) J. Biol. Chem. *267*, 3852−3861.
18. McIntosh, D. B., Parrish, J. C., and Wallace, C. J. A. (1996) J. Biol. Chem. *271*, 18379−18386.
19. Woods, A. C., Guillemette, J. G., Parrish, J. C., Smith, M., and Wallace, C. J. A. (1996) J. Biol. Chem. *271*, 32008−32015.
20. Wilson, M. T., and Greenwood, C. (1996) in *Cytochrome c: a multidisciplinary approach* (Scott, R. A., and Mauk, A. G., Eds.) pp 611−634, University Science Books, Sausalito.
21. Wallace, C. J. A. (1984b) Biochem J. *217*, 601−604.
22. Wallace, C. J. A., Corradin, G., Marchiori, F., and Borin, G. (1986) Biopolymers *25*, 2121−2132.
23. Wallace, C. J. A. (1984a) Biochem. J. *217*, 593−599.
24. Craig, D. B., and Wallace, C. J. A. (1995) Biochemistry *34*, 2686−2693.
25. George, P., and Tsou, C. L. (1952) Biochem. J. *50*, 440−448.
26. Craig, D. B., and Wallace, C. J. A. (1991) Biochem. J. *279*, 781−786.
27. Barker, P. D., and Mauk, A. G. (1992) J. Am. Chem. Soc. *114*, 3619−3624.
28. Ferrer, J. C., Guillemette, J. G., Bogumil, R., Inglis, S. C., Smith, M., and Mauk, A. G. (1993) J. Am. Chem. Soc. 115, 7507−7508.
29. Tsukihara, T., Aoyama, H., Yamashita, E., Tumizaki, T., Yamaguchi, H., Shinzawa-Itoh, K., Nakashima, R., Yaono, R., and Yoshikawa, S. (1996) Science *272*, 1136−1144.
30. Ramdas, L., and Nall, B. T. (1987) in *Abstracts of the UCLA Symposia*, Supplement to *J. Cell Biochem*. *218*.

BI971595M